

Laser cooling potassium for inter-species interaction study

Huang-Sheng Chiu
National Tsing Hua University

August 30, 2006

Abstract

Laser cooling potassium for inter-species interaction study

Master's dissertation

Huang-sheng Chiu

National Tsing Hua University, Taiwan

2006

Magneto-optical trap (MOT), producing high density and cold atoms, is an important implement to study atomic and molecular physics. A magneto-optical trap (MOT), capable of trapping K and Rb simultaneously, has been set up in our laboratory. The ^{39}K MOT was 10^9 atoms using a total laser power of 100 mW with a laser beam diameter of 1.2 cm. The system consist of a home-made Ti-sapphire laser, a commercial Ti-sapphire laser, a diode laser (DL100), an anti-Helmholtz coil, and the Ultra-High Vacuum system with potassium and rubidium getters. The mixture of the cold ^{39}K and ^{87}Rb MOT atoms is used for studying the interactions. Moreover, the interaction plays an important rule in formation of cold molecules. The inter-species collision loss was measured using the fluorescence. An absorption image is the next work for more accurate measurements. Moreover, the interaction between ^{41}K and ^{85}Rb , because of higher scattering length, will be researched.

Contents

1	Introduction	1
1.1	Overview	1
1.2	Motivation	1
1.3	Magneto-optical trapping	2
1.3.1	Doppler Cooling	2
1.3.2	Optical molasses	3
1.3.3	Magneto-optical trapping	3
2	Trapping ^{39}K	5
2.1	Energy levels of ^{39}K D2 transition	5
2.2	Stabilized titanium-sapphire laser	6
2.2.1	Single Mode Laser cavity	6
2.2.2	Single Mode Scanable setup	8
2.2.3	Frequency-modulated (FM) Saturated spectroscopy	10
2.2.4	Stabilization	13
2.3	Experimental setup	13
2.4	Number measurement	14
2.4.1	Method of number atoms	14
2.4.2	Results	17
3	Collisional loss in double-species MOT	21
3.1	Introduction	21
3.2	Experimental Setup	22

3.3 Result	22
4 conclusion	25

List of Figures

1.1	The atome absorbs and emits photons	2
1.2	Zeeman split in inhomogeneous magnetic field	4
2.1	Energy level diagram for potassium 39 D2 line	6
2.2	Ti-sapphire Laser cavity	7
2.3	picture of Ti:sapphire laser	7
2.4	Current driver scheme	8
2.5	Mechanical setup of etalon	9
2.6	figure of Ti:sapphire output monitor by scanning Fabry-Perot	9
2.7	The optical setup of FM spectroscopy of potassium D2 line	11
2.8	Saturated absorption spectroscopy of potassium D2 line	12
2.9	FM spectroscopy of potassium D2 line	12
2.10	Block diagram of Ti-sapphire laser locking scheme	13
2.11	The image and 3D picture of potassium MOT.	14
2.12	Schematic diagram for potassium MOT	15
2.13	The number of the ^{39}K MOT versus the detuning	18
2.14	Fluorescence of the MOT versus the laser intensity	19
2.15	Fluorescence of the MOT versus time in different vapor pressure.	19
2.16	Fluorescence of the MOT versus the magnetic flied gradient.	20
3.1	The image of the double MOT	23
3.2	Loading process of ^{39}K	24

List of Tables

2.1	The characteristic Data of D2 line of potassium 39[1]	5
2.2	Data of ^{39}K MOT with some parameters	18
3.1	Data of ^{39}K MOT with ^{87}Rb MOT or not	23
3.2	Data of ^{87}Rb MOT with ^{39}K MOT or not	23
3.3	The collision losses of ^{87}Rb MOT and ^{39}K MOT	23

Chapter 1

Introduction

1.1 Overview

In this chapter, I discuss the motivations of double species magneto-optical trap(MOT), potassium 39 and rubidium 87, and reviews of laser cooling. In Chapter 2, The home-made single frequency Ti:sapphire laser for potassium MOT and experimental parameters of ^{39}K MOT are discussed. Chapter 3, the observation of the mixture of ^{39}K and ^{87}Rb MOT and the measurement of the trap loss induced by collision between two species MOT are discussed. In the Chapter 4, we conclude the experimental results and future work.

1.2 Motivation

Laser cooling is a new technique to study atomic and molecular physics. The theory of laser cooling was proposed by Hänach and Schawlow in 1975[2]; Chu et al. created the first optical molasses in 1985[3], and then magneto-optical trap (MOT) was realized by Raab E.L et al. in 1987[4]. MOT is a powerful implement to create a novel physical phenomenon. Then, there are many species of MOT created in many labs in the world[5][6][7][8]. In addition, Bose-Einstein Condensate (BEC) was created by Anderson, M.H. et al and Davis, K.B. et al in 1995[9][10]. In 1998, cold molecules were produced using photoassociation by Fioretti, A. et al[11]. The molecular BEC

was brought to the world by Jochim S. et al. in 2003[12].

In this thesis, the ^{39}K MOT had been realized and the interaction between ^{39}K and ^{87}Rb was also discussed. We created a ^{39}K MOT and mixed it with ^{87}Rb MOT, and the characteristics of ^{39}K MOT and the trapping loss due to collisions of two species MOT are discussed. It is the pre-work for formation of heteronuclear cold molecules. There are many interesting applications of ultra-cold heteronuclear polar molecules, such as permanent dipole moment of electron, quantum degenerate behavior[13] and heteronuclear photoassociative spectroscopy[14]. It also can be applied to quantum computing[15].

1.3 Magneto-optical trapping

1.3.1 Doppler Cooling

When the atom absorbs a photon, it increases a momentum $\hbar\omega$ along the direction of photon. However, spontaneously emitting a photon in random direction makes the change of average momentum of the atom is zero.(see the figure.1.1). Therefore, the total change of momentum of atom is $\hbar\omega$. When the atom is interacting with red-detuned photons, it only absorbs the photons coming form the opposite direction of it velocity, because of the Doppler effect. It gains a momentum $-\hbar\omega$ and it is decelerated by the light.

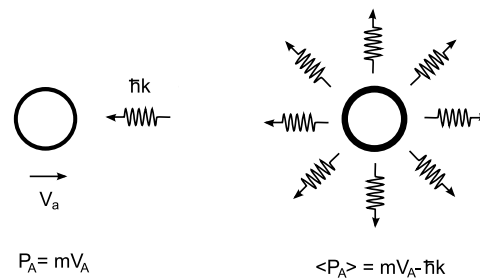


Figure 1.1: The momentum of the atom after absorbing a photon and then the spontaneous emission, P_A is the momentum of atom.

1.3.2 Optical molasses

If there are three pairs of counter-propagating lights in three orthogonal directions, they form an isotropic deceleration region in the intersection[3]. Atoms moving along all directions would be decelerated in this region, and this phenomenon is the so-called optical molasses. However, optical molasses only decelerates atoms, rather than traps atoms in a place.

1.3.3 Magneto-optical trapping

The method of trapping atoms exploits magnetic field and Zeeman-shift to confine atoms in a place[4]. In a two-level system, assuming that the ground state is $S = 0 (m_s = 0)$ and the upper states are $S = 1 (m_s = -1, 0, \text{and } 1)$ Zeeman splitting is position-dependent in an inhomogeneous magnetic field ($B(Z) = bZ$) (see figure.1.2). The energy shift is $\Delta E = \mu m_s B = \mu b m_s Z$. If there is a pair of opposite circular polarized lasers propagating in the counter-direction (see fig.(1.2)), the atoms in $Z < 0$ would have a higher probability to absorb photons with a velocity directed to $Z=0$. On the other hand, the atoms in $Z > 0$ have a higher probability to absorb photons with a velocity directed to $Z=0$. The reason is that the atoms in the $Z < 0$ have a higher probability to absorb σ^- photon than σ^+ due to the selection rule, vice versa. Therefore, the atoms are trapped in the point of $Z=0$.

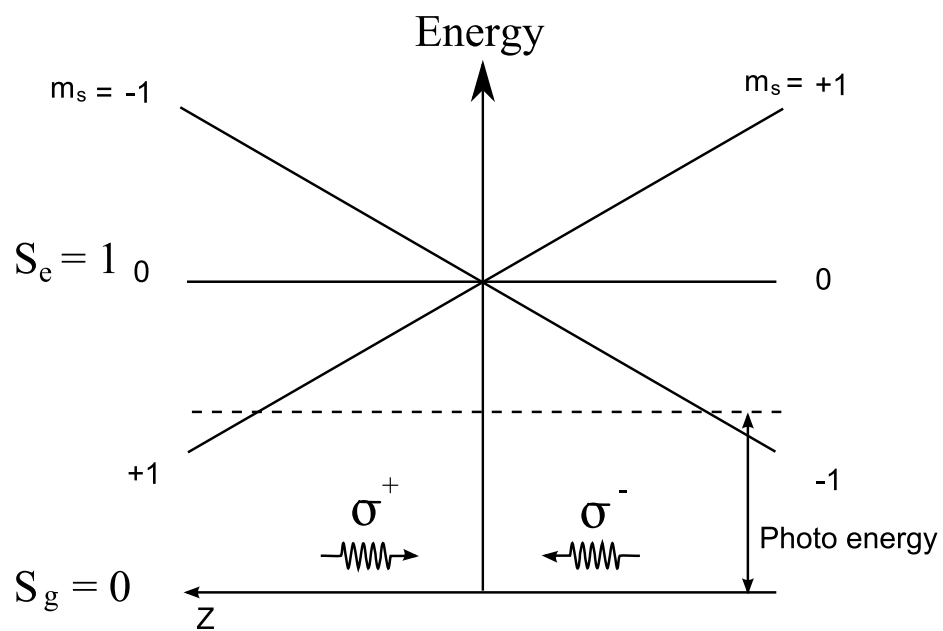


Figure 1.2: Zeeman split in inhomogeneous magnetic field

Chapter 2

Trapping ^{39}K

2.1 Energy levels of ^{39}K D2 transition

The natural abundance of potassium 39 is 93.3 percent and the isotope potassium 41 is 6.7 percent. The MOT of potassium 39 had been firstly created using D2 of transition of ^{39}K for cooling atoms. The ground-state hyperfine splitting is 462MHz for ^{39}K . The hyperfine structures of ^{39}K D2 transition can not provide a good close loop for cooling atoms, because 34MHz of the upper levels splitting of ^{39}K D2 transition is too small. The typical laser cooling configuration is: The laser is red-detuned to $4\text{S}_{1/2}(F = 2) \rightarrow 4\text{P}_{3/2}(F = 3)$. Then, the laser is also blue-detuned to $4\text{S}_{1/2}(F = 2) \rightarrow 4\text{P}_{3/2}(F = 0, 1 \text{ and } 2)$. Therefore, to solve such a problem, the frequency of laser was tuned below all hyperfine levels of $4\text{P}_{3/2}$. In this case, the spontaneous transitions from upper levels are possibly not only to $4\text{S}_{1/2}(F = 2)$ but also to $4\text{S}_{1/2}(F = 1)$. Therefore, another laser with a frequency of $4\text{S}_{1/2}(F = 1) \rightarrow 4\text{P}_{3/2}$ is necessary to avoid that the all atoms are pumped to $4\text{S}_{1/2}(F = 1)$ state and it also cool the atoms. Trapping and Repumping transitions are indicated in the fig.(2.1) and the characteristic parameters of ^{39}K are in table (2.1)

Atom	transition	I	λ (nm)	$\hbar\omega_a$ (eV)	τ (ns)	$\gamma/2\pi$ (MHz)
^{39}K	$4\text{S}_{1/2}-4\text{P}_{3/2}$	3/2	766.70	1.1617	26.31	6.09

Table 2.1: The characteristic Data of D2 line of potassium 39[1]

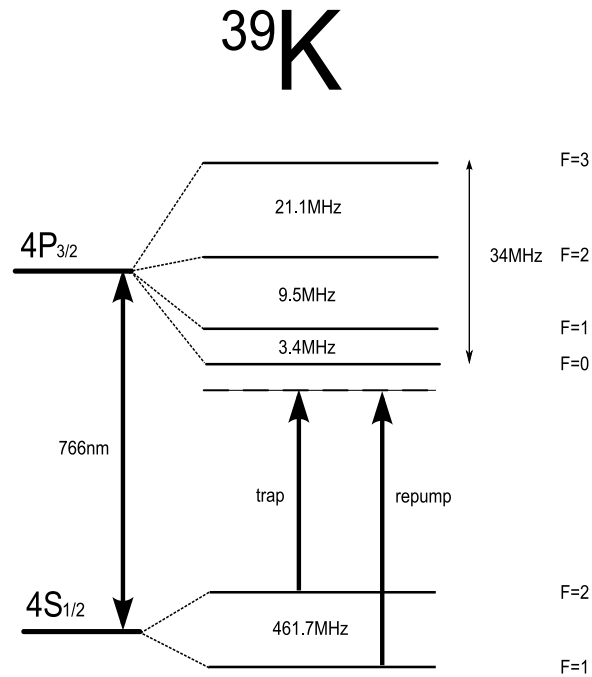


Figure 2.1: Energy level diagram for potassium 39 D2 line

2.2 Stabilized titanium-sapphire laser

2.2.1 Single Mode Laser cavity

A high power and frequency stabilized laser source about 766 nm is necessary for a stable ^{39}K MOT. The home-made Ti-sapphire laser pumped by the DPSS CW pump laser (Verdi-6, coherent) was used to the main laser source.(see fig.(2.3)). Its free spectral range (F.S.R) of the ring cavity was about 254 MHz. There are two lasing directions in the ring cavity, therefore an optical diode inside the cavity is to achieve uni-direction lasing. The gain spectrum of Ti-sapphire is form 0.6 μm to 1 μm . Coatings of cavity mirrors, a Lyot filter, and an intra-cavity thin etalon were used for single mode lasing. First, the high reflection coating of 650-800nm confine laser output frequency such a coating range. Second, the Lyot filter reduces bandwidth to \sim nm, and it can tune frequency by rotating about the axis normal to the crystal face. Finally, the thin etalon selects only one of all the cavity modes.

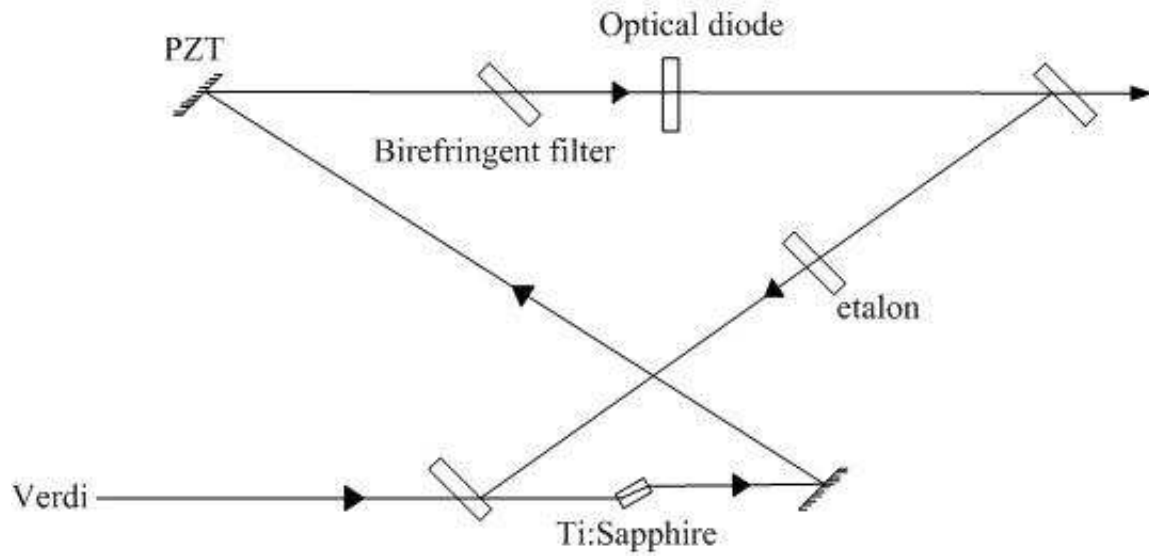


Figure 2.2: Ti-sapphire Laser cavity

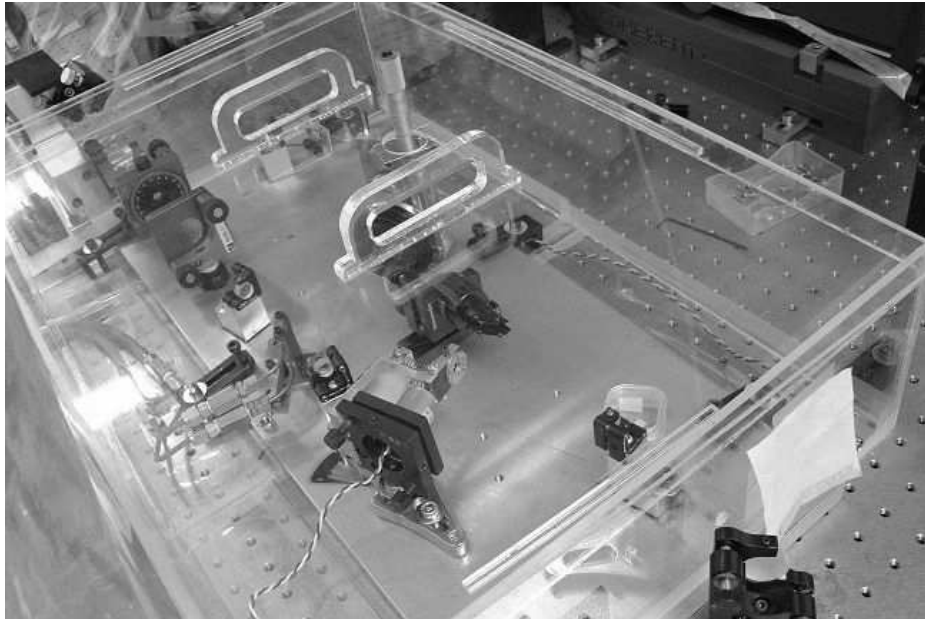


Figure 2.3: picture of Ti:sapphire laser

2.2.2 Single Mode Scannable setup

The frequency of Ti-sapphire laser in our lab was scanned by moving one of cavity plan mirror with peizo. To prevent mode hopping, the thin etalon angle should move synchronously with the peizo. When a function of signal $s(t)$ is sending to peizo, we generate another signal $s_1(t) = a + bs(t)$ by the electric circuit. $s_1(t)$ was forwarded to current driver (see fig.(2.4)) to control the angle of the thin etalon. The thin etalon is mounted on a static system with two springs(see fig.(2.5)). When the current drives is entering the motor, the angle of thin etalon rotates to a new static state. a and b was adjusted to optimal values to avoid mode hopping. The Ti-sapphire laser is able to scan about 1-2 G Hz continuously without mode hopping at 766nm.

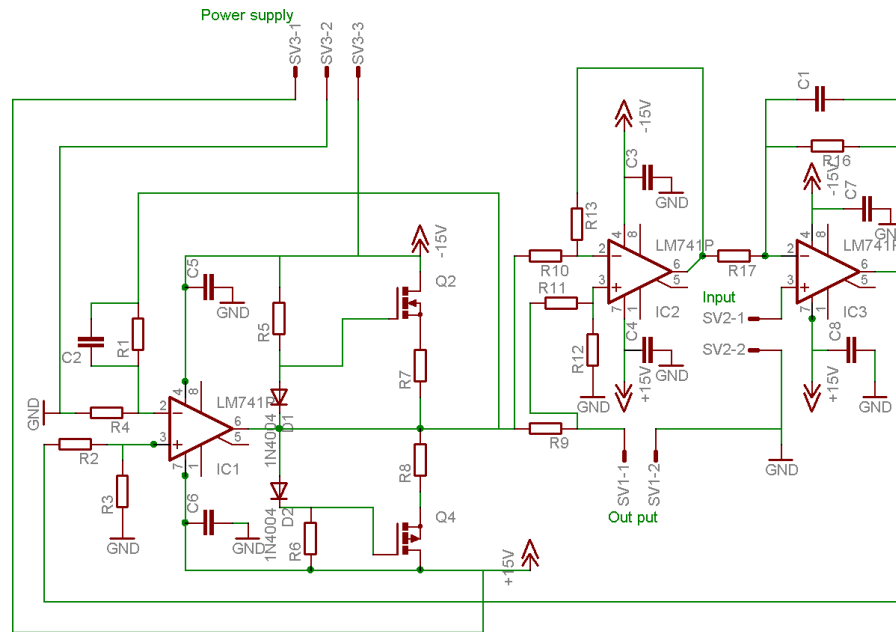


Figure 2.4: Current driver scheme

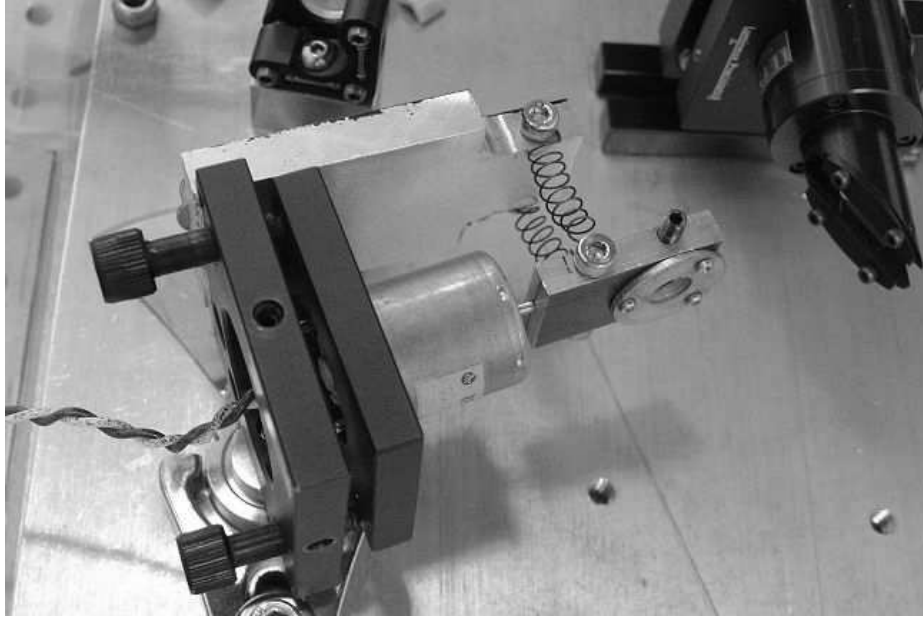


Figure 2.5: Mechanical setup of etalon

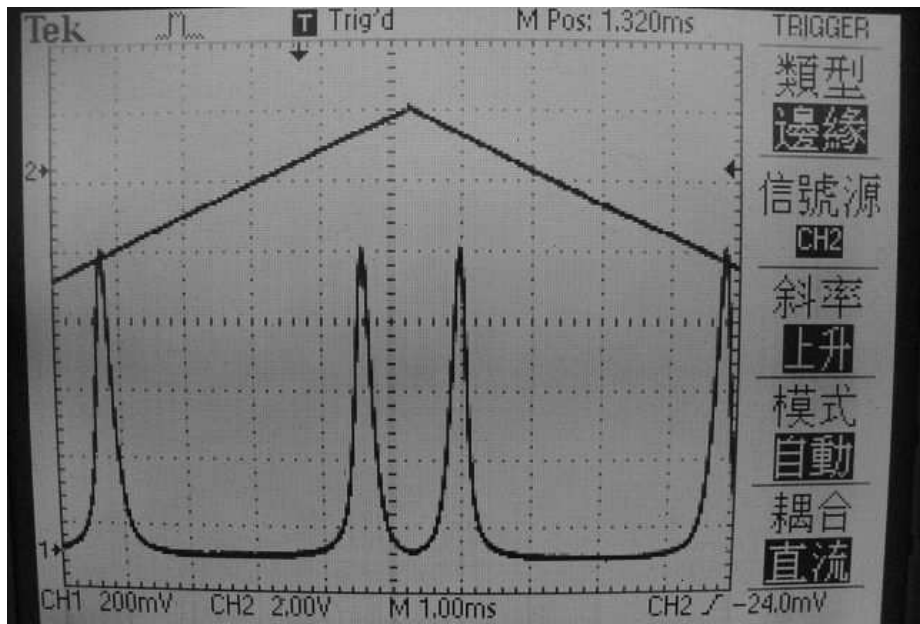


Figure 2.6: figure of Ti:sapphire output monitor by scanning Fabry-Perot

2.2.3 Frequency-modulated (FM) Saturated spectroscopy

The accuracy of laser frequency has to be stabilized better than 1 MHz for producing a stable MOT. Therefore, the Ti-sapphire laser should be pick-locked on a Doppler-free spectrum. First step, the zero and first order laser beams passing AOM with the frequency shift +231 MHz are used in the Doppler-free spectroscopy. The optical setup and saturation spectroscopy are shown in fig.(2.7) and (2.8) schematically.

Second step, an EOM (Electro-Optic Modulator) is applied to generate the frequency modulation spectroscopy. The EOM with the modulation frequency ω_m phase modulates a laser beam to produce sideband at $\omega \pm n\omega_m$. ω_m should be the resonance frequency of the EOM for enhancing the modulation. The main frequencies we care about are $n = 0$ and ± 1 because their amplitudes are much larger than others. The probe beam with the frequencies $\omega \pm n\omega_m$ combines with the saturated beam in potassium cell, and the beats of the probe beam are detected by a photodiode. The beat notes between ω and $\omega \pm \omega_m$ and between ω and $\omega - \omega_m$ are demodulated by DBM with reference frequency ω_m . And then it is secondly demodulated by lock-in amplifier. The optical setup and spectroscopy saturated absorption spectroscopy are shown in fig.2.7 and fig.2.9 schematically

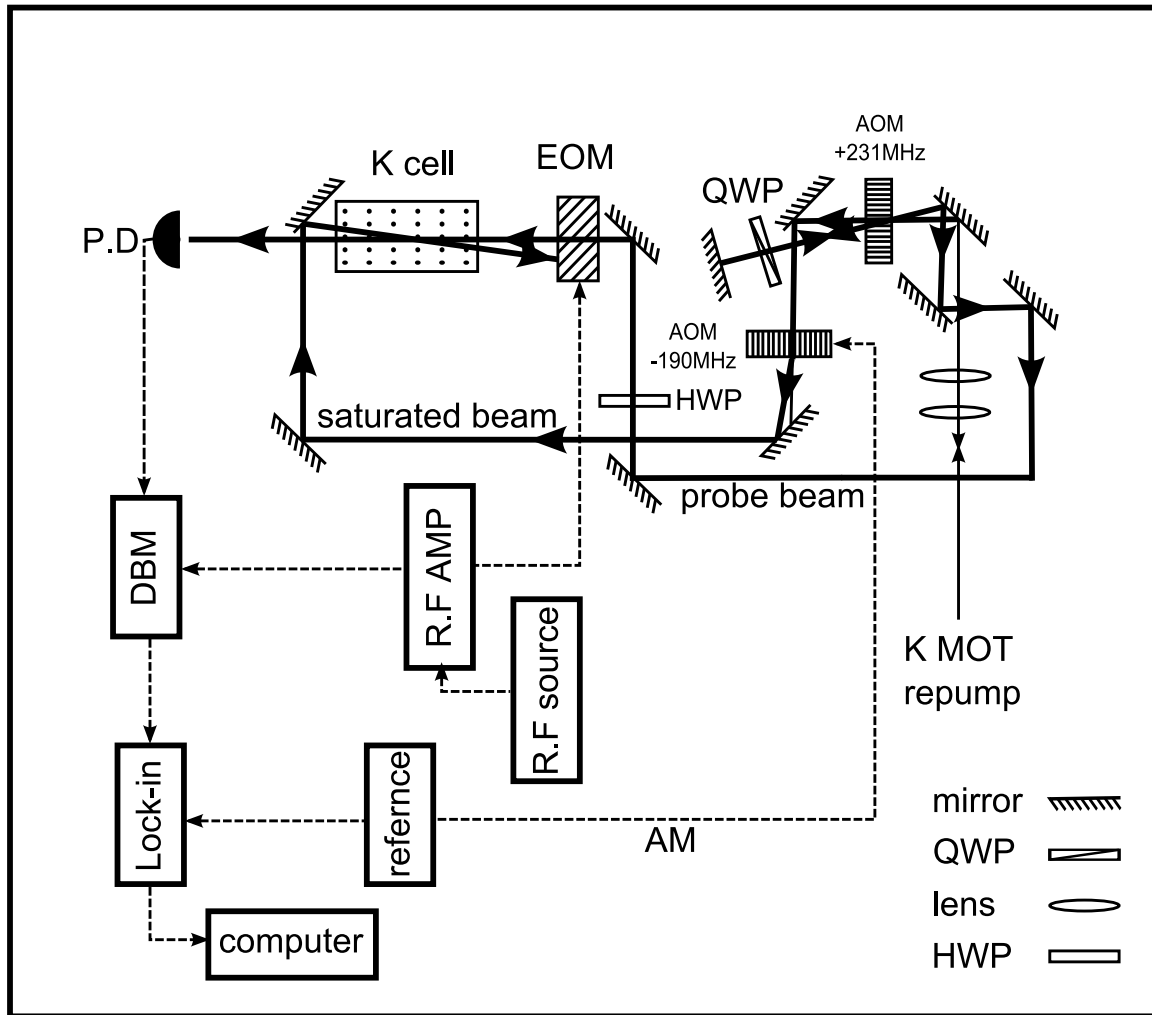


Figure 2.7: The optical setup of FM spectroscopy of potassium D2 line

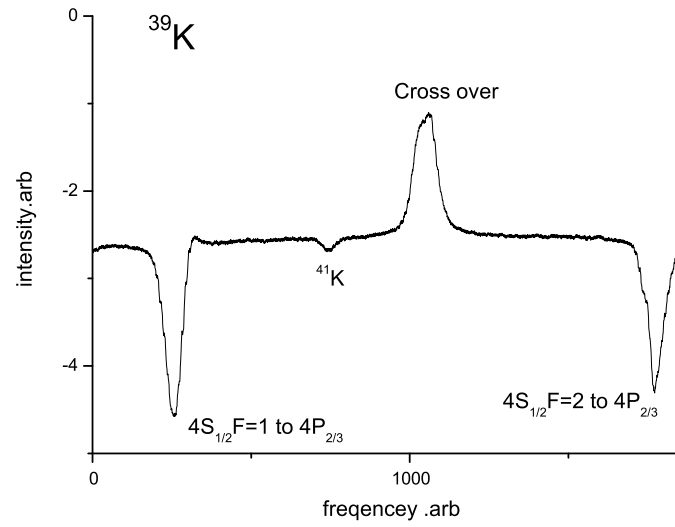


Figure 2.8: Saturated absorption spectroscopy of potassium D2 line

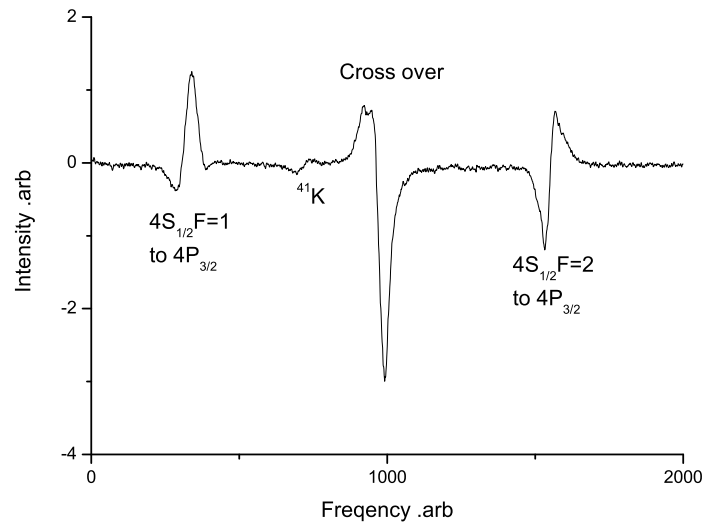


Figure 2.9: FM spectroscopy of potassium D2 line

2.2.4 Stabilization

The error signal in F.M spectroscopy is used to lock laser frequency and it is delivered to PID(proportional-integral-differential feed back loop). The signal from the PID was then sent to a high voltage amplifier and the etalon simultaneously. The high voltage amplifier can control the length of the piezo of the mirror. The system can provide a fixed laser frequency, and be fine-tuned by varying the frequency of the offset AOM. The detail procedures are illustrated as fig.(2.10).

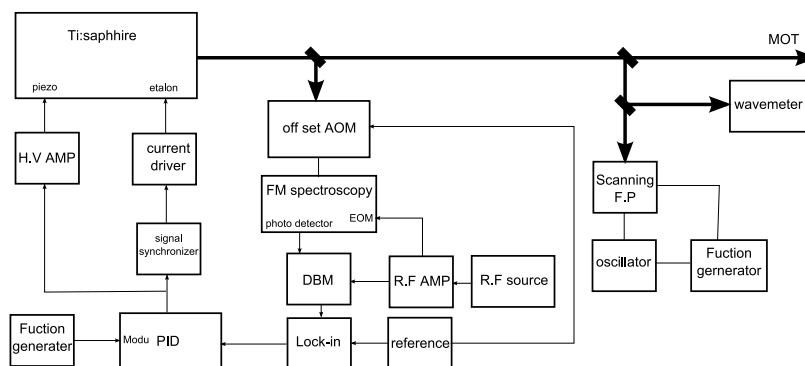


Figure 2.10: Block diagram of Ti-sapphire laser locking scheme

2.3 Experimental setup

A stainless steel chamber with potassium and rubidium getters provides a ultra-vacuum system pumped to 10^{-10} torr and was placed between anti-Helmholtz coils. The home-made Ti:sapphire laser provides the light to ^{39}K MOT, which is set red to the transition, $4S_{1/2}(F = 2)$ to $4P_{3/2}$. Pure nitrogen gas is filled into laser cavity to avoid the absorption of O_2 at 766nm. The light is split by PBS(polarization beam splitter), and passes a double AOM at +231 MHz as the repump light. The lasers were then split into three parts, x ,y and z directions, by several PBSes and half-wave plates. The intensity ratio of laser is about 1:2:1.5 for compensating rubidium MOT laser beam because the deviation of polarizations among potassium trap, potassium repump and rubidium trap lasers are about 10 degrees. The six beams intersect at

the zero point of magnetic field . Finally, formation of the MOT was observed using CCD Camera. The image of ^{39}K MOT and the optical system is diagrammed in fig.(2.11)and fig.(2.12).

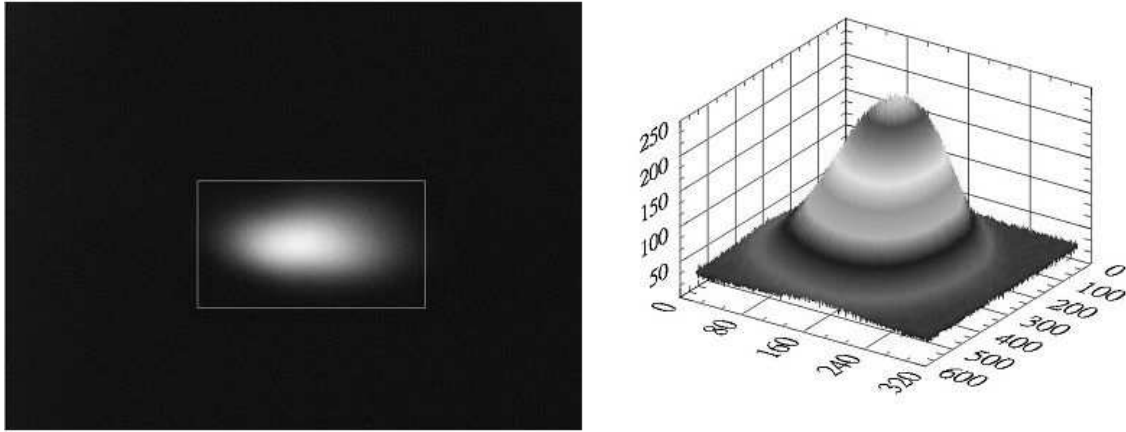


Figure 2.11: The image and 3D picture of potassium MOT. The MOT size is $3.22\text{mm}\times 1.93\text{mm}$ ($1/e^2$)

2.4 Number measurement

2.4.1 Method of number atoms

There are six zeeman sublevels involving cooling mechanism at ^{39}K MOT(see fig.(2.1)). In order to calculate the number of potassium atoms using fluorescence image, the population at all upper states has to be estimated[16].

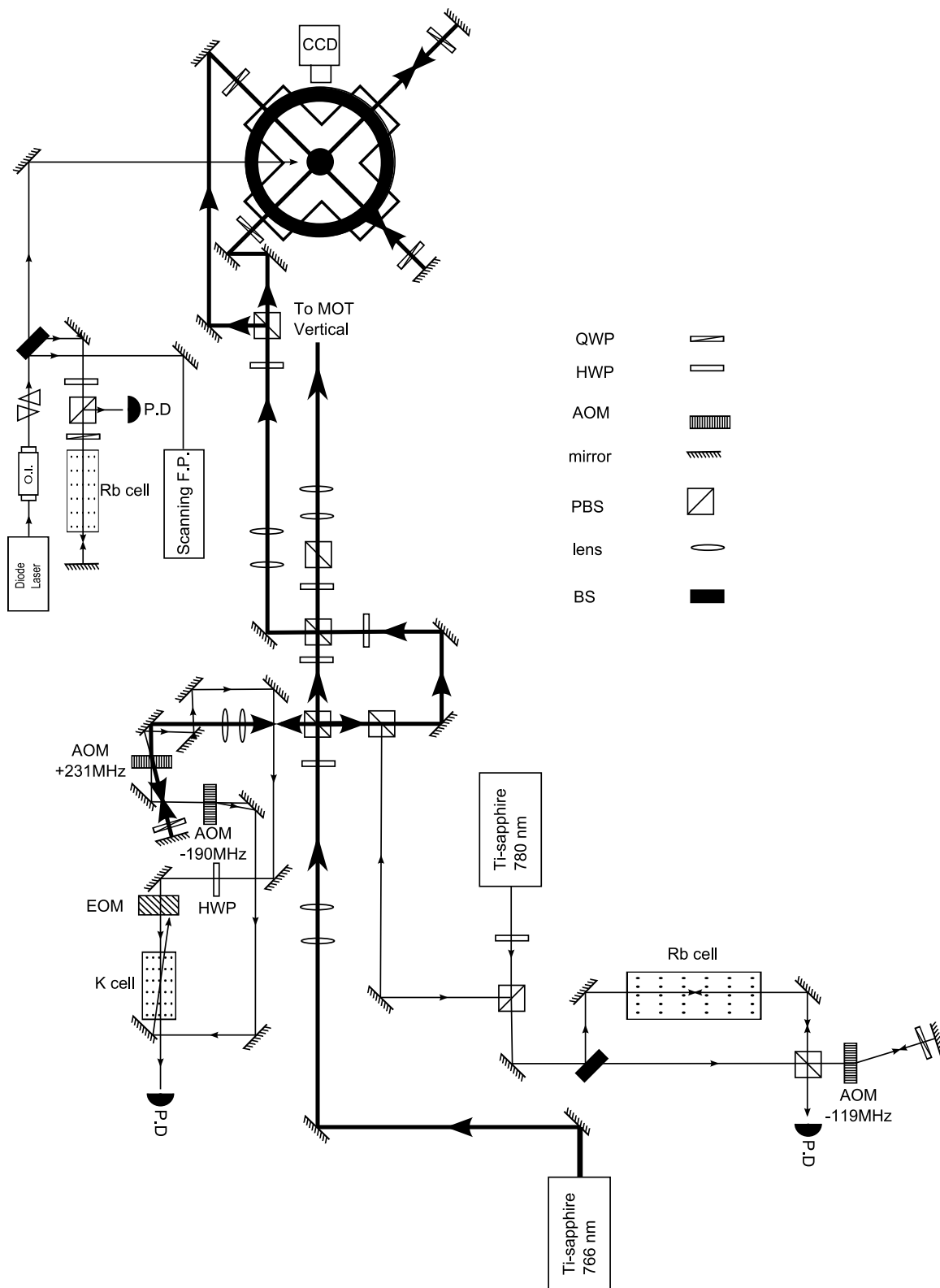


Figure 2.12: Schematic diagram for potassium MOT

The rate equation for the population of each of the upper-state level is

$$\dot{p}_F = R_{F1}(p_1 - p_F) + R_{F2}(p_2 - p_F) - \Gamma p_F \quad (2.1)$$

Here, $p_f = p_1, p_2$ is the population of lower states population and p_F is the populations of upper states. R_{Ff} is the exciting rate between F to f . F is upper states and f is lower states. $\Gamma = 1/2\pi\tau$. τ is life time of upper state.

The lower state populations is

$$\dot{p}_f = \sum_F [R_{Ff}(p_F - p_f) + \Gamma_{Ff}p_F] \quad (2.2)$$

where $\Gamma_{Ff} = b_{Ff}\Gamma$, b_{Ff} is the branching ratio from F to f .

The excitation rates R_{Ff} between F and f is

$$R_{Ff} = \frac{c_{Ff}\Gamma_{Ff}}{2} \left(\frac{I_f/I_s}{1 + 4(\frac{\nu_f - \nu_{Ff}}{\Gamma})^2} \right) \quad (2.3)$$

Here the coefficient c_{Ff} is oscillator strength and ν_{Ff} is transition frequency between F and f . I_f and ν_f are laser intensity and frequency. I_s is the saturation intensity.

In steady states, $\dot{p}_F = \dot{p}_f = 0$, so we can get

$$p_F = \frac{R_{F1}p_1 + R_{F2}p_2}{R_{F1} + R_{F2} + \Gamma} \quad (2.4)$$

$$p_f = \frac{\sum_F (R_{Ff} + \Gamma_{Ff})p_F}{\sum_F R_{Ff}} \quad (2.5)$$

Combining eq.(2.4) and eq.(2.5) we can get p_2 in term of p_1 :

$$p_2 = \frac{\sum_F \frac{R_{F2} + \Gamma_{F2}}{R_{F1} + R_{F2} + \Gamma} R_{F1}}{\sum_F \frac{R_{F1} + \Gamma_{F1}}{R_{F1} + R_{F2} + \Gamma}} p_1 \quad (2.6)$$

Assigning $p_1 = 1$, we can calculate p_2 , and then get all upper states p_F by using eq.(2.4). We normalize all level population and sum all upper states p_F to get ρ_e , the

normalized populations of all upper state.

$$\rho_e = \frac{\sum_F p_F}{\sum_f p_f + \sum_F p_F} \quad (2.7)$$

When we get ρ_e , the number of atoms of ³⁹K MOT can be given by

$$N_{atom} = \frac{E_d \tau}{\Omega E_\gamma \rho_e} \quad (2.8)$$

Here, E_γ is the photon energy of the potassium D2 transition and Ω is solid angle collection fraction. E_d is detecting power of the CDD camera. For get E_d , we calibrate power at one pixel value in CCD picture. The total power provide by calibrating all pixel value.

2.4.2 Results

Some experimental data of MOT are present as following. First, we measure the number of the atoms of ³⁹K MOT by varying the detuning frequency of trap and repump laser. In fig. (2.13), the maximal value of the number occurs when the detuning is 2Γ , Γ :natural linewidth of the D2 transition. Next, we observed the fluorescence versus I_{trap} and I_{repump} in fig. (2.14). When the ratio to trap and repump lasers is about 1 : 0.8, it is more efficient to cool the atoms. It is because that the ratio of the probability $F = 2$ to $F = 1$ as $4P_{3/2}$ dropping $4S_{1/2}$ is nearly to 1 : 0.8.

The fluorescence of the MOT process under different background vapor pressure is illustrated in fig 2.15. The fluorescence was increased by the vapor pressure, and no saturation was observed. In addition, we observed the fluorescence with various magnetic gradient as fig.(2.16), and found its maximum at 7 Gauss/cm. The ³⁹K MOT was 10^9 atoms using a total laser power of 100 mW with a laser beam diameter of 1.2 cm. The diameter of MOT is 1.6mm \times 0.94mm.

	Max. ^{39}K MOT atoms
Detuning from $4P_{3/2}(F=0)$	2Γ
Ratio of trap and repump laser	1 : 0.8
Vapor pressure	10^{-9} torr
B field gradient	7 Gauss/cm

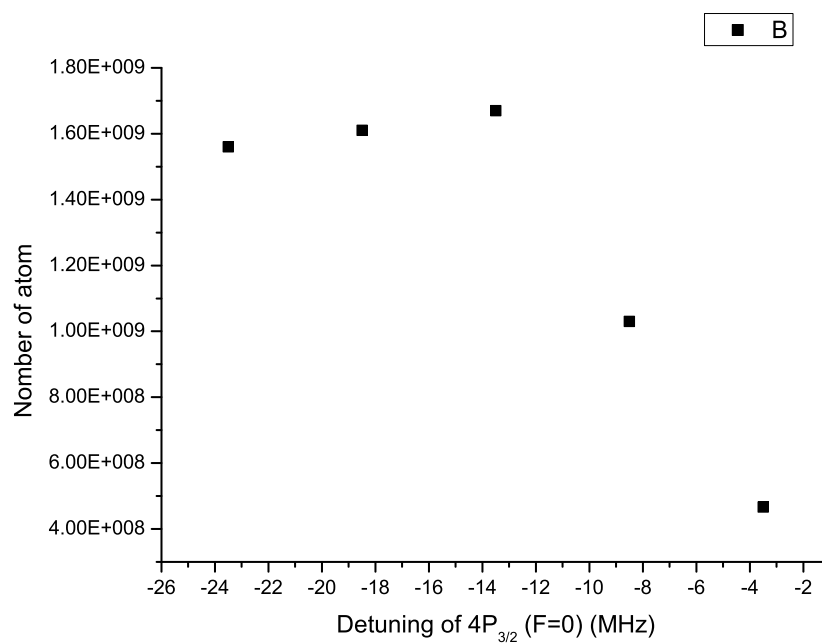
Table 2.2: Data of ^{39}K MOT with some parameters

Figure 2.13: The number of potassium atoms in the MOT versus the detuning of hyperfine structure $4P_{3/2}(F=0)$. Data are taken with intensity $I_{trap} = 41.5(\text{mW}/\text{cm}^2)$ and $I_{repump} = 38.5(\text{mW}/\text{cm}^2)$. The gradient of magnetic field was 14 (Gauss/cm)

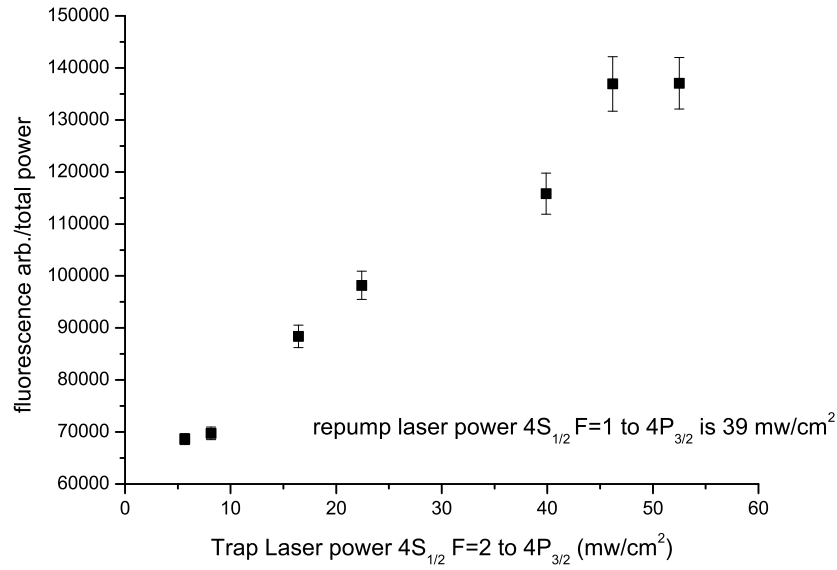


Figure 2.14: Fluorescence in the MOT versus the laser intensity I_{trap} , and $I_{repump} = 53\text{mW}$. The detuning of 1Γ , natural linewidth of $4P_{3/2}$, from $4P_{3/2}(F=0)$. The gradient of magnetic field was 15 (Gauss/cm)

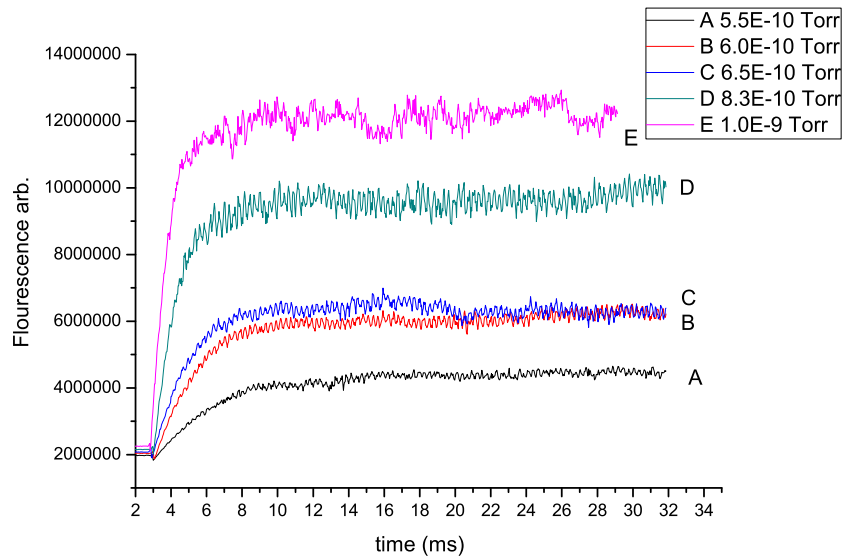


Figure 2.15: Fluorescence in the MOT as a function of time in different vapor pressure. Data are taken with intensity $I_{trap} = 46(\text{mW}/\text{cm}^2)$ and $I_{repump} = 34(\text{mW}/\text{cm}^2)$. The detuning of 1Γ , natural linewidth of $4P_{3/2}$, from $4P_{3/2}(F=0)$. The gradient of magnetic field was 15 (Gauss/cm)

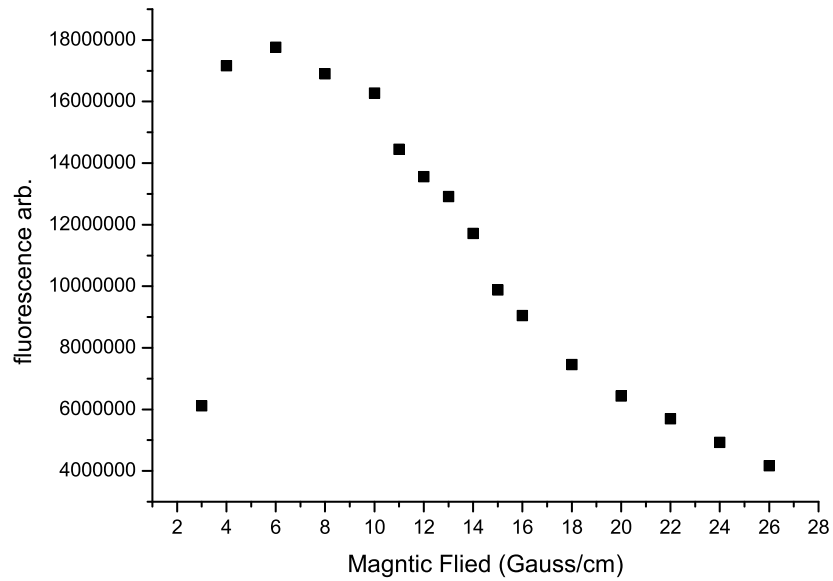


Figure 2.16: Fluorescence in the MOT versus the magnetic field gradient. Data are taken with intensity $I_{trap} = 46(\text{mW}/\text{cm}^2)$ and $I_{repump} = 34(\text{mW}/\text{cm}^2)$. The detuning of 1Γ , natural linewidth of $4P_{3/2}$, from $4P_{3/2}(F = 0)$. The gradient of magnetic field was $15(\text{Gauss}/\text{cm})$

Chapter 3

Collisional loss in double-species

MOT

3.1 Introduction

A double species MOT, high density and cold atomic gas, is a method to produce cold molecules. Collisions play an important rule in the process of atoms to molecules. The collision loss between potassium and rubidium MOT is a clear phenomenon to observe the interactions of double-species MOT. The rate equation would be used to calculate collision loss between potassium and rubidium MOT. The rate equation of potassium in rubidium MOT is [17]

$$\frac{dN_K}{dt} = L - \gamma N_K - \beta n_K N_K - \beta' n_{Rb} N_K \quad (3.1)$$

Where L is loading rate, γ is the collision loss rate between the atoms of ^{39}K and hot background gas. β is the loss rate in ^{39}K itself, and β' is the loss rate due to the collision between ^{39}K and ^{87}Rb . Assuming n_K is constant in the process of formation[18][19], the solution of eq.(3.1) is

$$N_K = N_0 \{1 - \exp[-(\gamma + \beta n_K + \beta' n_{Rb})t]\} \quad (3.2)$$

$N_0 = L/(\gamma + \beta n_{Rb} + \beta' n_K)$ is the number of potassium MOT in steady-state. By measuring the fluorescence in a process of formation of K MOT and fitting the data to eq.(3.2), the loading time of MOT can be found. When Rb MOT exists, $\gamma + \beta n_K + \beta' n_{Rb}$ can be measured. Without Rb MOT, we can measure $\gamma + \beta n_K$. By subtracting $\gamma + \beta n_K + \beta' n_{Rb}$ from $\gamma + \beta n_K$, $\beta' n_{Rb}$ was extracted. If n_{Rb} is measured, β' would be found.

3.2 Experimental Setup

The optical diagram is show in fig.(2.12). The Ti:sapphire Laser about 780nm is the trap laser for ^{87}Rb MOT. A little part of the laser is used to rubidium FM saturation absorption spectroscopy for locking at the peak of transition $5S_{1/2}(F = 2)$ to $5P_{3/2}(F = 3)$ red detuned by 14 MHz. The repump laser is provide by diode laser (DL 100), locked at the transition $5S_{1/2}(F = 2)$ to $5P_{3/2}(F = 2)$. In order to generate two spices MOT in the same place, we combine rubidium trap laser with potassium trap and repump lasers by PBS. The repump laser of ^{87}Rb is sent to MOT by another channel, because it only transports $5S_{1/2}(F = 1)$ to $5S_{1/2}(F = 2)$, no cooling effect. Finally, the image is recorded by a CCD camera. It is shown as fig.(3.1). The ^{87}Rb MOT is on the right side and the ^{39}K MOT is on the left side.

3.3 Result

One of the MOT processes and fitting data are as fig.(3.2). In this case, the laser intensity I_{trap} and I_{repump} is 46.5 and 35 mW/cm². The magnetic gradient is 15 Gauss/cm. The data of ^{39}K MOT and ^{87}Rb MOT is listed as the tab.(3.1) and tab.(3.2). The n_{Rb} was 5×10^{10} /cm³ and then the β' was 2.5×10^{-12} cm³/s. For rubidium, the n_K was 3×10^{11} /cm³ and β' was 2.1×10^{-13} cm³/s. The entire data is shown in table.(3.3)

⁸⁷ Rb MOT	N ₀ of ³⁹ K MOT (arb. Unit)	$\gamma + \beta n_K$	$\gamma + \beta n_K + \beta' n_{rb}$
without	5.71×10^6	1.427/s	—
with	4.50×10^6	—	1.553/s

Table 3.1: Data of ³⁹K MOT with ⁸⁷Rb MOT or not

³⁹ K MOT	N ₀ of ⁸⁷ Rb MOT (arb. Unit)	$\gamma + \beta n_{Rb}$	$\gamma + \beta n_{Rb} + \beta' n_K$
without	5.64×10^6	0.325/s	—
with	4.65×10^6	—	0.388/s

Table 3.2: Data of ⁸⁷Rb MOT with ³⁹K MOT or not

	density of atoms n	$\gamma + \beta / \text{cm}^3$
³⁹ K MOT	3×10^{11}	2.5×10^{-12}
⁸⁷ Rb MOT	1×10^{10}	2.1×10^{-13}

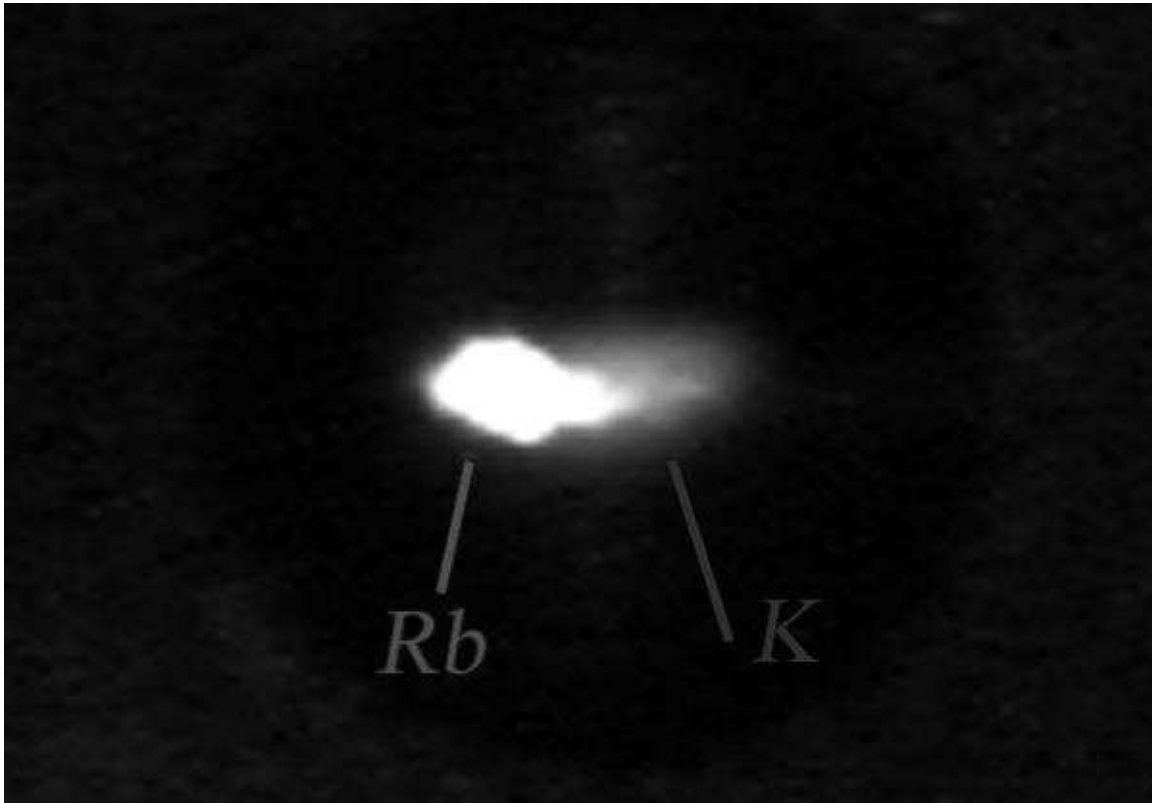
Table 3.3: The collision losses of ⁸⁷Rb MOT and ³⁹K MOT

Figure 3.1: The image of the double MOT

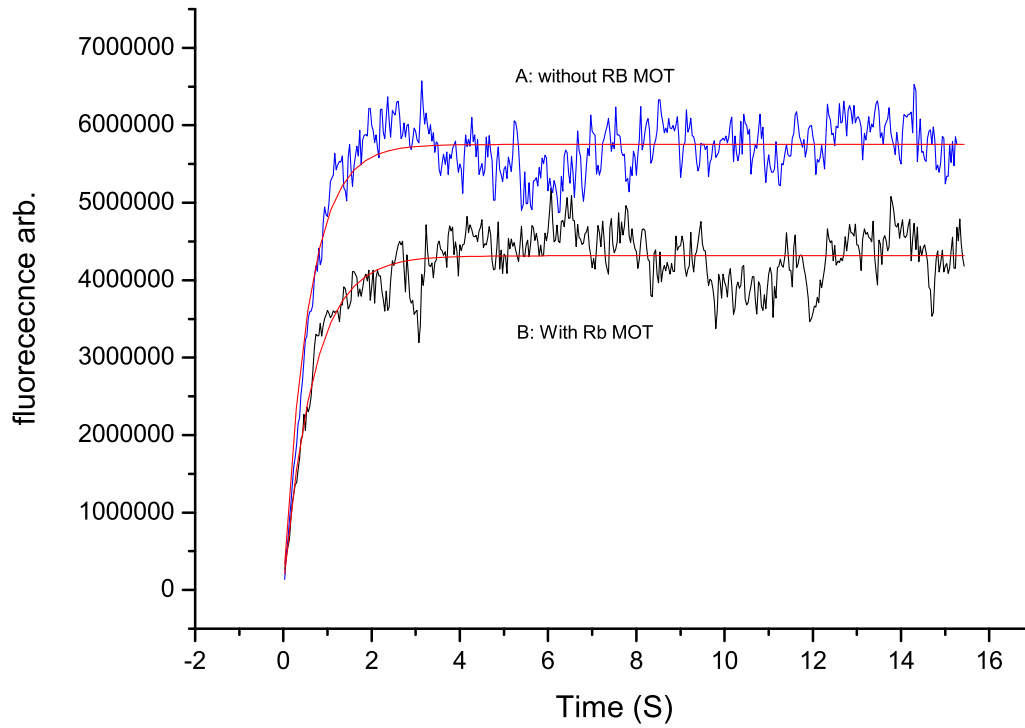


Figure 3.2: Loading process and fitting data with rubidium MOT and without rubidium MOT.

Chapter 4

conclusion

A ^{39}K MOT that had 10^9 atoms with a size of $1.6\text{mm}\times 0.94\text{mm}$ has been observed in our lab. It can be mixed with ^{87}Rb MOT by combining two optical setups. However, it is difficult to overlap two MOTs. The reason is that our image system is difficult to observe the entire 3D distribution of the MOT. Another CCD camera should be set up. In addition, the number of the cold ^{39}K atoms is unstable, and fluctuates about 20% of the saturation. It could be caused by the instability of the laser. In addition, the mixture of the double-MOT had been observed and the collision losses of two species in the MOT help us to understand the interaction of the atoms. The losses might result from the Radiative escape (RE), fine-structure (FC) and hyperfine-structure-changing collision (HCC), and Gallagher-Pritchard Model should be improved to deal with the problem[20].

Future work

In the future, possible works for improvements in this experiment are listed below:

- The laser system and optical setup will be improved for the more stable MOT.
- A compensative coil will be used to the Polarization-Gradient cooling.
- An absorption image system can measure the temperature and the number of atoms accurately.

- The isotope ^{41}K and ^{85}Rb MOT may be mixed for their higher scattering length.

References

- [1] H. J. Metcalf and P. van der Straten, *Laser Cooling and Trapping* (Springer-Verlag New York Inc., New York, 1999).
- [2] T. Hansch and A. Schalow, *Opt. Comm.* **13**, 68 (1975).
- [3] S. Chu *et al.*, *Phys. Rev. Lett.* **55**, 48 (1985).
- [4] E. L. Raab *et al.*, *Phys. Rev. Lett.* **59**, 2631 (1987).
- [5] N. W. M. Ritchie *et al.*, *Phys. Rev. A* **51**, R890 (1995).
- [6] C. D. Wallace *et al.*, *Phys. Rev. Lett.* **69**, 897 (1992).
- [7] R. S. Williamson III and T. Walker, *J. Opt. Soc. Am. B* **12**, 1393 (1995).
- [8] D. Sesko *et al.*, *Phys. Rev. Lett.* **63**, 961 (1989).
- [9] M. H. Anderson *et al.*, *Science* **269**, 198 (1995).
- [10] K. B. Davis *et al.*, *Phys. Rev. Lett.* **75**, 3969 (1995).
- [11] A. Fioretti *et al.*, *Phys. Rev. Lett.* **80**, 4402 (1998).
- [12] S. Jochim *et al.*, *Science* **302**, 2101 (2003).
- [13] L. Santos, G. V. Shlyapnikov, P. Zoller, and M. Lewenstein, *Phys. Rev. Lett.* **85**, 1791 (2000).
- [14] H. Wang and W. C. Stwalley, *J. Chem. Phys.* **108**, 5767 (1998).
- [15] D. DeMille, *Phys. Rev. Lett.* **88**, 067901 (2002).
- [16] R. S. Williamson III, Ph.D. thesis, University of Wisconsin-Madison, 1997),.
- [17] M. S. Santos *et al.*, *Phys. Rev. A* **52**, R4340 (1995).
- [18] T. Walker, D. Sesko, and C. Wieman, *Phys. Rev. Lett.* **64**, 408 (1990).
- [19] L. Marcassa *et al.*, *Phys. Rev. A* **47**, R4563 (1993).
- [20] A. Gallagher and D. E. Pritchard, *Phys. Rev. Lett.* **63**, 957 (1989).